Analyst

Accepted Manuscript

ROYAL SOCIETY OF CHEMISTRY

www.rsc.org/analyst

Mass spectrometric imaging of *in vivo* protein and lipid adsorption on biodegradable vascular replacement systems

*Sophie M. Fröhlich[1], Magdalena Eilenberg[2,3], Anastasiya Svirkova[1], Christian Grasl[3,4], Robert Liska[5], Helga Bergmeister[2,3], Martina Marchetti-Deschmann[1]**

1) Institute of Chemical Technologies and Analytics, Vienna University of Technology, Vienna, Austria
2) Division of Biomedical Research, Medical University Vienna, Vienna, Austria
3) Ludwig Boltzmann Cluster for Cardiovascular Research, Vienna, Austria
4) Center for Medical Physics and Biomedical Engineering, Medical University Vienna, Vienna, Austria
5) Institute of Applied Synthetic Chemistry, Vienna University of Technology, Vienna, Austria

*) Corresponding Author:
Assoc.-Prof. Dr. Martina Marchetti-Deschmann
Austria – 1060 Vienna, Getreidemarkt 9/164-IAC
T: +43 – 158851 – 15162, F: +43 158801 – 915162
E: martina.marchetti-deschmann@tuwien.ac.at

Abstract

Cardiovascular diseases present amongst the highest mortality risks in Western civilization and are frequently caused by arteriosclerotic vessel failure. Coronary artery and peripheral vessel reconstruction necessitates the use of small diameter systems that are mechanically stress-resistant and biocompatible. Expanded polytetrafluorethylene (ePTFE) is amongst the materials used most frequently for non-degradable and bio-degradable vessel reconstruction procedures, with thermoplastic polyurethanes (TPU) representing a promising substitute. The present study describes and compares the biological adsorption and diffusion occurring with both materials following implantation in rat models. Gel electrophoresis and thin-layer chromatography, combined with mass spectrometry and mass spectrometry imaging, were utilized to identify the adsorbed lipids and proteins. The results were compared with the analytes present in native aorta tissue. It was revealed that both polymers were severely affected by biological adsorption after 10 min *in vivo*. Proteins associated with cell growth and migration were identified, especially on the luminal graft surface, while lipids were found to be located on both the luminal and abluminal surfaces. Lipid adsorption and cholesterol diffusion were found to be correlated with the polymer modifications identified on degradable thermoplastic urethane graft samples, with the latter revealing extensive cholesterol adsorption. The present study demonstrates an interaction between biological matter and both graft materials, and provides insights into polymer changes, in particular, those observed with thermoplastic urethanes already after 10 min *in vivo* exposure. ePTFE demonstrated minor polymer modifications, whereas several different polymer signals were observed for TPU, all were co-localized with biological signals.

Keywords: vascular replacement system, expanded polytetrafluorethylene, thermoplastic polyurethanes, protein, lipid, mass spectrometry imaging, MALDI

Graphical Abstract:

INTRODUCTION

Cardiovascular diseases have extremely high prevalence and are the greatest source of mortality in Western European countries and in the United States.[1] Coronary artery and peripheral vascular pathological issues often necessitate the partial or total replacement of vessel systems. A large variety of solutions have been developed, including using cellular and polymer materials that are used to create either degradable or non-degradable artificial vessels.[2, 3] Reproducible production, high biocompatibility and extreme mechanical adaptability are all requirements of artificial vessels that are met by polymer-based graft systems.[4]

Small-diameter vascular vessel systems are particularly important in bypass surgery and vascular-reconstruction procedures.[5, 6] Expanded polytetrafluorethylene (ePTFE) has an inert microporous fibrous structure, has frequently been used in vascular-replacement procedures, especially when autologous tissue is unavailable, and no *in vivo* degradation of ePTFE has been observed in studies conducted to date.[7] However, FTIR analysis has revealed significant protein interactions and, in particular, lipid uptake that correlates with implantation time and patient-related risk factors.[8, 9] The use of ePTFE for clinical coronary bypass applications is currently avoided owing to low patency.[10, 11] Thermoplastic polyurethanes (TPU) are well established for use in biomedical applications because of their high bio and blood compatibility, and owing to their efficient adaptability to mechanical forces, both of which are properties that are similar to natural tissues. If accurately designed, TPU vessels provide a thriving biodegradable alternative for vascular replacement.[12, 13] However, thrombus formation is a crucial limitation for these materials and the interactions between polymer materials and the biological environment has not been described in detail, even though it clearly impacts material modification and improvement.[14] To our knowledge only one study is available showing the impact of polymer surface and structure, pH of the enviroment and molecular weights and pIs of the model proteins on their adsorption on thermoplastic elastomeric surfaces.[15] We present for the first time results from in vivo experiments and moreover not only for proteins but also lipids.

Mass spectrometry imaging (MSI) has been successfully established as a technique for characterizing polymer surfaces and their interactions with bio-compartments.[16-18] This technique presents an opportunity to obtain information about both the polymer and potential reactive biological compounds on the molecular level.[15, 19] In the current study, polymer-based replacement systems for small-diameter vessels are studied with respect to their interactions with the biological surrounding. The objective of the work performed in this study was to better understand polymer degradation and/or replacement mechanisms occurring on the molecular level; it was of interest

because biological adsorption and diffusion are assumed to initiate the favourable biodegradation and replacement processes.[20-23] It was of interest to establish a method that can be used to directly access the differences in protein and lipid adsorption between degradable and non-degradable polymer materials, and to gain information on molecular modifications affecting the polymer in one approach. Since MSI itself is not a method for unambiguous identification, interacting analytes were characterized following extraction by using polyacrylamide gel electrophoresis (PAGE) and thin layer chromatography (TLC) techniques, followed by mass spectrometry (MS). A functional analysis of identified proteins in combination with classified lipid structures provides the ability to obtain detailed information regarding the adsorption process and facilitates the suggestion of possible material improvements.

MATERIALS AND METHODS

All chemicals and reagents, unless otherwise indicated, were purchased from Sigma-Aldrich (USA) with a purity of at least 99%. Ultra-pure water (uH_2O) was obtained using a Simplicity system (Millipore, USA) with 18.2 MΩ×cm resistivity at 25°C.

Polymer grafts and animal model

ePTFE prostheses were purchased (Zeuss, Orangeburg, South Carolina, USA) and used as control. Biodegradable TPU grafts were synthesized and electrospun as described.[24, 25] Both materials were sterilized with ethylene oxide before implantation into the infra-renal aorta of 12 inbred Sprague Dawley rats (male, bodyweight 300–400 g)[26]. Following graft ectomy, samples were washed with isotonic sodium solution to remove functional clots and were immediately put on dry ice for transportation and storage. The animal studies were conducted in compliance with protocols approved by the Ethical Committee for Animal Research of the Medical University of Vienna and the Austrian Federal Ministry of Science and Research. All graft samples (ePTFE and TPU) were analysed with respect to their lipid and protein interactions after 10 minutes and 7 days exposure *in vivo*. Samples from three independent animal experiments were used. Native aorta and rat blood were extracted from rats after explant surgery at the Institute of Biomedical Research (Medical University Vienna, Austria); these samples were used for biological reference.

MS profiling and MS imaging

The scheme depicted in Fig. 1 illustrates the areas investigated using MSI. Cut samples (> 4 mm in order to analyse the affected and non-affected areas in the same MSI experiment) were attached onto indium tin oxide (ITO)-coated glass slides (Bruker Daltonics, Germany) using a conductive tape. For the purposes of cross-section analysis, explanted graft materials were stabilized in optimal cutting temperature (O.C.T. TissueTek) embedding medium and sliced to a thickness of 10 µm using a microtome (Reichert-Jung, Germany). All samples were washed using 0.1% TFA for lipid analysis and uH_2O for protein analysis, before being vacuum dried. For the matrix-assisted laser desorption/ionization time-of-flight mass spectrometry (MALDI-TOF-MS) and MSI analysis of proteins, standard MALDI matrices, sinapic acid (SA, 25 mg/mL) and ferulic acid (FA, 20 mg/mL) were dissolved in acetonitrile (ACN) and ethanol, both containing aqueous 0.1% TFA, before being mixed 6/3 (v/v). Lipid analysis was performed using a 20 mg/mL solution of 2,4,6-trihydroxyacetophenone (THAP) in KCl-saturated methanol. Matrix deposition was performed using a chemical inkjet printer (ChIP-1000, Shimadzu Kratos Analytical, Japan) and an airbrush device (Conrad, Germany), the latter had a working distance of 10–12 cm, at an angle of approx.. 50–60°, covering the sample in several iterative steps. MS profiling and MSI experiments were performed on an UltrafleXtreme III (Bruker Daltonics) in positive ion mode with linear or reflectron detection, applying a laser repetition rate of 2 kHz. Samples were rastered at a spatial resolution of 15–150 µm (details are given in the respective sections of the manuscript), mass spectra were acquired over an average sample size of 125 mm^2 (approx. 15 × 8 mm) for all samples if not stated otherwise. The laser beam size was set to “small” or “medium” for MSI analysis, and to “minimum” for graft-wall analysis (*i.e.* cross-section). The images produced were based on 1000 laser shots per position for lipid analysis and 2000 laser shots for proteins. For image reconstruction, FlexImaging v3.0 (Bruker Daltonics) was used. All MSI data sets were presented as median normalized but were also verified for outliers and artefacts using root mean square and total ion current normalization.

Principal Component Analysis (PCA)

PCA was performed by applying Clinprotools v2.2 (Bruker Daltonics) on the acquired profiling spectra. 73 features were selected for the differentiation of peptides in the sample and 38 features for lipid-based differentiation. Both models were cross validated.

Protein analysis

For the purpose of protein extraction, exactly 4 mm of graft material was maintained in 1200 µL of uH_2O before 100 µL of trichloracetic acid (20 % in uH_2O) was subsequently added five times, with the sample being vortexed thoroughly before each addition. Samples were incubated for 30 min at 4°C and were centrifuged at 14000 rpm at 4°C for another 30 min. The polymer material was removed, the supernatant was discarded and the pellet was re-dissolved in 10 µL uH_2O before the protein concentration was determined using the Bradford protein assay method.[27] To perform SDS-PAGE analysis, protein pellets were dissolved in sample buffer (26.5 mM Tris HCl, 35.25 mM Tris Base, 0.5% lithium dodecyl sulfate, 2.5% glycerol, 0.1275 mM EDTA, 0.055 mM SERVA Blue G250, 0.044 mM Phenol Red, pH 8.5, 50 mM dithiothreitol) at 95°C for 5 minutes before being applied to a precast NuPAGE 4–12% Bis-Tris polyacrylamide gel (Life Technology, USA). Electrophoresis was conducted at a constant voltage (125 V) in an XCell Surelock Mini Cell (Life Technology). All samples were loaded with the same amount of protein, 2 µg (+/- 8 %, n = 3). Protein identification after *in-gel* digestion, MS and MS/MS analysis was performed as previously described[16] on the instrument described above. In brief, after excising the gel lane and removing the silver staining the sample was reduced, alkylated and trypsinized. After overnight digestion, peptide extraction and micro-purification the peptides were applied onto a stainless steel target together with α-cyano-4-hydroxy-cinnamic acid (CHCA, 5 mg/mL in 50 % acetonitrile containing 0.1 % trifluoroacetic acid). For all enzymatic digestion data, autolytic tryptic products, keratin and gel blank artefacts were assigned and removed before database search (Swissprot, January 2014) using Mascot.[28] The database search was performed with the following parameters: taxonomy *Rattus norvegicus*, monoisotopic mass values, peptide mass tolerance of ±0.3 Da (for peptide mass fingerprint (PMF) and peptide sequencing), two missed cleavages, carboxyamidomethylation as fixed modification and methionine oxidations as variable modification. A protein was considered to be correctly identified if the following criteria applied: significant MASCOT score for PMF or at least three fragmentation experiments (MS/MS), generated in LIFT mode without collision gas, correlated with the biological and molecular mass information.

Lipid analysis

For the purpose of lipid extraction, exactly 4 mm of graft material was incubated in 900 µL of chloroform/methanol (2:1, v/v) for 1 h at room temperature. 450 µL of chloroform and 450 µL of uH_2O (1:1, v/v) were added sequentially before the sample was subjected to centrifugation

at 3000 rpm at room temperature for 15 min. The organic phase was collected and evaporated under vacuum conditions. As a reference sample, 20 µL of rat blood and 4 mm of rat aorta tissue (not homogenized) were treated as described above. For further analysis, dried lipids were dissolved in 15 µL of chloroform. Lipid separation was conducted by HP-TLC analysis. 8 µL of chloroform extract was applied to the Silica gel 60 HP-TLC aluminium plates (10 × 10 cm, 0.2 mm layer thickness, particle size 3–4 µm from Merck, Germany) with a syringe. HP-TLC separation was performed using repeated development with increasing migration distances. First development: 65-70 % of the sample-loaded plate was developed with solvent system A (methyl acetate/1-propanol/chloroform/methanol/aqueous saturated potassium chloride, 25/25/25/10/0.5, v/v/v/v/v) to separate glycolipids from phospholipids. The HP-TLC plates were dried with a heat gun. Second development: 95 % of the plate was developed in solvent system B (toluene/diethyl ether/ethanol/acetic acid, 60/40/1/0.05, v/v/v/v) for neutral lipid separation. For lipid visualisation, the HP-TLC plates were stained with 0.05 % primuline in acetone/uH_2O (8/2, v/v) and the lipid spots were detected at a wavelength of 337 nm. The monomer material used for the TPU grafts were analysed in the same manner after dissolving 0.5, 1 and 10 mg in 1 mL chloroform. For MALDI-TOF-MS analysis again 20 mg/mL THAP dissolved in potassium chloride (KCl) saturated methanol was used. The lipid sample and matrix solution were mixed 1/1 and 1 µL was deposited on a stainless steel target (Bruker Daltonics). MALDI mass spectra were acquired on the UltrafleXtreme III in the positive ion, reflectron detection mode. For performing MALDI-TOF-MS analysis from HP-TLC plates directly, a developed plate was mounted on a TLC adapter (Bruker Daltonics) and THAP (20 mg/mL) in acetone was deposited using a pipette on the identified areas of lipid spots. Lipids were characterized after LIFT mode fragmentation without collision gas. The MS/MS window was set to 0.7 % to observe characteristic head group signals for all lipid classes, *i.e.* sphingomyelins, phosphatidylcholines and lysophosphatidylcholines (m/z 184), phosphatidylserines (m/z 105), phosphatidylethanolamines (m/z 125) and phosphatidylinositols (m/z 299). Characteristic neutral losses from the head group were used to decipher sphingomyelins from (lyso-)phosphatidylcholines. Cholesterol identification is also based on characteristic fragmentation. Instrument parameters and spectra interpretation were previously described in further detail.[29]

RESULTS AND DISCUSSION

Protein analysis directly from graft materials

MALDI-linear TOF profiling was performed directly on graft samples covered with SA/FA matrix to analyse the intact, adsorbed proteins (Fig 2a,b). Protein patterns on the luminal and abluminal surfaces revealed comparable m/z values for both, TPU and ePTFE materials. Comparability in this term is considered as similar pattern regarding homogeneity/heterogeneity of analyte distribution and comparable MS spectra during profiling experiments for 3 analysed samples. In general, it can be said that the observed m/z values were similar to those of pure blood plasma, which was applied directly on the glass slide as a reference sample. Signals between m/z 2000 and 80000 were registered. If the majority of signals are considered to be singly charged molecular ions, which cannot be proven currently owing to the available resolving power of the mass analyser, the pattern distributions correlate to the SDS-PAGE findings (details see later) and protein names were tentatively assigned in Fig. 2b. For both graft materials and time points, protein signals were of significant higher quality for the luminal surfaces in terms of the signal intensity, signal-to-noise ratio and especially reproducibility.

PCA was performed in order to differentiate ePTFE and TPU, time points and/or localizations. Although the number of biological replicates is not significant yet, these first results show that certain m/z pattern were characteristic for the luminal and abluminal surfaces for both polymers (Fig. 2c) and the polymer type was clearly distinguished (Fig. 2d). The *in vivo* time of ePTFE could not be classified using PCA, however, this might be a consequence of the low signal intensities. For TPU it was possible to obtain a good differentiation of 10 min and 7 d *in vivo*. In particular, proteins relevant for classification were found in the mass range between m/z 3000 and 18000.

Despite significant chemical differences for both graft materials and the supposed biological inertness and hydrophobicity of ePTFE, which is the golden standard for non-degradable materials, it is obvious that biological interaction takes place for both materials already after short *in vivo* time spans.

Protein localization by MSI

Intact protein localization was based on MSI experiments. Polymer graft sections were analysed as described and compared to aorta tissue, which was utilized as a standard native vessel material. For all samples, the high-salt concentration had to be reduced by carefully washing with uH_2O followed

by performing vacuum evaporation. The hydrophobic surface parameters of the grafts required the deposition of very small matrix droplets to avoid analyte diffusion. In combination with an increased matrix concentration, a very thin seeding matrix layer (SA/FA) was applied first, using the ChIP-1000 to support efficient analyte incorporation and matrix homogeneity. The printed seed layer was subsequently covered by carefully applying thin consecutive layers of the same matrix solution with an airbrush. The latter technique deposited the higher quantities of matrix necessary for an efficient MALDI process within a reasonable time while preserving homogeneous crystallization.

Fig. 3 illustrates the visualization of intensity values for three exemplary analytes adsorbed on the luminal and abluminal ePTFE surfaces (10 min *in vivo*). TPU samples revealed similar results for intact proteins. Furthermore, the distribution of the same m/z values in native aorta tissue is presented. Despite careful washing procedures, light microscopy images revealed blood residues on the transition region from the graft to the blood vessel. Additionally, material fringing from the cutting process can be observed in Fig. 3 at edge "a" of the rectangular shaped material. Aorta tissue was observed to provide a very homogeneous but almost transparent tissue surface.

For some analytes, very distinct areas of adsorption were observed. m/z 16100, most likely corresponding to the $[M+H]^+$ of the haemoglobin subunits, was found to be particularly prevalent in areas correlated with blood residues. The identified regions affected by adsorption demonstrated either long drawn out shapes or a homogeneous distribution on the luminal surface. The abluminal graft surface reveals two highly affected areas of protein adsorption. m/z values indicate these to be haemoglobin and lipoprotein or lipoprotein subunits (m/z 16100, 3200 and 6500), and less specific distributions of albumin (m/z 66000) and other proteins (for the latter data are not shown). The clearly defined areas indicate contact or interaction with the surrounding tissue during implantation that might have resulted in increased protein adsorption.

Comparing the lateral distribution of the proteins after 7 days *in situ*, revealed very homogeneous protein adsorption patterns covering the whole graft area. Proteins in the higher mass range, *e.g.* albumin, were distributed very homogeneously for both time points.

Protein analysis after extraction from graft materials

Wide-ranging information about proteins interactions with the graft materials was obtained by extracting proteins from the graft materials after 10 min and 7 days *in vivo*. Sample-to-sample differences were observable in the protein patterns obtained by SDS-PAGE after loading 2 µg of protein for each sample (Fig. 4). These differences were considered as significant as protein pattern for sample replicates (explants from different time points) were reproducible. Varying band

intensities were found from the analysis of the TPU and ePTFE extracts after 10 min, but the protein patterns were rather similar. These differences were mainly considered as biological variation, which needs to be further minimized in future work. Despite the hydrophobic nature of ePTFE, comparable protein patterns in terms of analyte distribution and profiling spectra were observed after short *in-situ* times. However, it can be seen that the *in-vivo* time affects protein adsorption on both polymer types. After 7 days, the signal intensities decreased and high molecular weight proteins were found to be dominant. Interestingly, for all proteins no obvious differences in the presence of protein were observed between the centroid and transition regions of the blood vessel graft materials for both time points.

Highly abundant blood proteins were identified alongside proteins associated with cell and muscle growth. This may indicate that the initial degradation and replacement process includes cell-layer formation; however, this may also be associated with thrombic platelet formation. That protein adsorption was observed after only 10 min *in vivo* on the centre and the edges of the graft demonstrates that protein interactions with the polymer occur immediately after implantation, and that the complete blood vessel implant from one end to the other is affected. This is in good agreement with the observation that the colour of the graft immediately changes into red indicating blood flow through the graft walls.[31] This study is not raising claim to fully cover the absorbed proteome, yet it is remarkable that in addition to highly abundant blood plasma proteins, several proteins with low concentrations were identified (Fig. 2). In comparison with the complete blood proteome, a rather low number of proteins was identified from the graft extracts. Three main reasons were considered to be relevant: (a) the high proportion of water in blood represses protein adsorption onto the hydrophobic polymer material, especially for hydrophilic proteins; (b) the constant blood flow counteracts adsorption by carrying proteins away from the polymer surface before they adhere; and (c) the interaction between graft material and blood components is most likely based on adhesion effects and, consequently, only the highly adhesive protein fraction will attach to the polymer quickly enough before being carried away. Therefore, it can be considered that proteins associated with cell growth and/or aggregation are preferentially adsorbed onto the polymers alongside serum albumin, a well-known carrier protein with strong adherence potential. It has also to be mentioned at this point that no growth factor was identified after SDS-PAGE. The reason for this is the study design which was not intended to give access to low abundance-proteins but to visualize the differences for the most abundant proteins. Based on the results from SDS-PAGE, both the hydrophilic and hydrophobic materials interacted in a similar manner with proteins in the blood; however, absorption of blood components between 50–70 kDa, *e.g.* albumin and fibrinogen, was favoured, in particular, by ePTFE after 7 days.

Lipid localization by MSI and polymer modifications

In addition to the analysis of protein components, lipids were also of interest because of their capacity to modify polymers owing to their oxidation and radical formation properties during metabolism, and their significant contribution to flow properties and adsorption. Lipid distributions on the grafts were studied and in the case of cholesterol, the diffusion pattern into the graft wall was also investigated. Again a seeding film of matrix, THAP dissolved in methanol, was applied on the graft surfaces using the ChIP-1000, followed by THAP (dissolved in ethanol) application by airbrushing.

Polymers are usually easily desorbed and ionized during the MALDI process. Therefore, the use of laser energies above a certain limit lead to intensive polymer background signals, especially in the mass range relevant for lipids, between m/z 600 and 2000. Consequently, the laser fluence (energy delivered per unit area) had to be adjusted carefully for each matrix combination and polymer, considering laser-induced carbon cluster formation from the polymer as an indicator for too much energy being used. The smallest possible laser step size, corresponding to the approximate laser diameter of the applied Smartbeam II laser, was above 30 µm for the ePTFE and 150 µm for the TPU samples, resulting in good S/N ratios for lipids and no signal background from the polymers (laser diameter set to "small" and "medium"). Contrary to the findings with protein adsorption, lipids were distributed homogeneously after only 10 min *in vivo* (Fig. 5). In comparison with the TPU samples, ePTFE revealed poor signal resolution and weaker intensities, possibly owing to ion suppression effects occurring during the desorption/ionization process or the higher insulating properties of ePTFE (disadvantageous for desorption/ionization process). The exemplarily visualized phospholipids (PC[18:1/13:0], PC[20:4/14:1]) formed a recognizable layer on the luminal surface of graft vessels after 10 min *in vivo*, which transformed into a more homogeneous layer after 7 days. After both time points, polymer distributions (Δm/z 254 for TPU and 137 for ePTFE) were detected, locally correlating with lipid adsorption. ePTFE, which was observed to be far less affected by molecular degradation, revealed one case of severe polymer modification, which was co-localized with lipid signals. The observed homogeneous lipid distribution does not allow further conclusions to be drawn, except for the fact that lipids interact significantly with both materials.

Polymer degradation behaviour and material replacement is theoretically affected, if not initiated, by molecule diffusion processes. Consequently, the diffusion of lipids into the materials is highly interesting, especially for biodegradable materials. Based on our experiences with ultrahigh molecular weight polyethylene (UHMW-PE) in interaction with biological fluids and literature,[16, 32] especially the diffusion of cholesterol into TPU was studied. The thickness of the vessel wall, less

than 100 µm (TPU: wall thickness 78 ± 10 µm and 1.6 mm inner diameter; ePTFE: 98 ± 10 µm and 1.5mm inner diameter), necessitated very careful sample treatment and preparation in order to perform proper MSI experiments. Graft cross-sections mounted on ITO slides were washed with uH_2O to remove salts and embedding medium. A matrix was applied as described for the lipid MSI surface analysis and experiments were performed at 15 µm lateral resolution (laser set to "minimal", which corresponds to a diameter of approximately 8 µm; measured under light microscope after ablation). Cholesterol ($[M\text{-}H_2O+H]^+$ m/z 369), the major component demonstrating high prevalence for, and interaction with, polymer based implants, was observed to diffuse into the TPU construct (Fig. 6). Areas of high cholesterol were visualized in the graft vessel wall; this was interpreted as a consequence of the TPU pore size favouring the diffusion of small molecules. It is hypothesized that this further increases the diffusion of other molecules (also other lipids), leading to enhanced cell aggregation, resulting in decreased thrombosis prevalence.

Lipid analysis after extraction from graft material

The analytical strategy used for protein analysis was adapted to globally investigate lipid classes. Information about the present lipids adsorbed on the graft materials was obtained following lipid extraction. Extracts from both polymers, ePTFE and TPU, both time points, 10 min and 7 days, and both regions, luminal and abluminal, were compared to extracts from native rat aorta and blood. To distinguish between lipids and eventually dissolved polymer, the monomer used for TPU synthesis was dissolved in chloroform at different concentrations and also applied to HP-TLC analysis. Fig. 7 shows the results for 4.5, 8 and 80 µg TPU monomer. To estimate completeness of extraction, samples from continuing extraction steps were also applied. Latter did not exhibit spots on the HP-TLC which led to the conclusion that the extraction procedure was rather complete and that no polymer was solubilized from the grafts during the incubation with chloroform (data not shown). After HP-TLC separation, lipids were characterized from the TLC plate using MALDI-TOF-MS analysis and MS/MS fragmentation for the determination of the head group (lipid class) and acyl chain length distribution (Fig. 7 gives a summary of the identifications). HP-TLC analysis showed for the first time the presence of all biologically relevant lipid classes on the graft material: glycerophosphatidylcholine (PC), lysophosphatidylcholine (LPC), sphingomyelin (SM), glycerophosphatidylserine (PS), glycerophosphatidylinositol (PI), glycerophosphatidylethanolamine (PE), cholesterol, triglycerides (TG), ceramides and several unspecified apolar glycolipids.

When compared with the native blood and aorta tissue, ePTFE revealed a very similar lipid pattern after an incubation time of only 10 min. However, TPU demonstrated extensive cholesterol traces (marked with * in Fig. 7) and analytes, which did not migrate with the mobile phase and remained at the application point. In polymers, not supposed to degrade or be replaced over time, Cholesterol adsoprtion is assumed to loosen the polymer matrix, enhancing lipid diffusion and protein adsorption[33].

The remains at the point of application are polar lipid species (e.g. glycolipids, lipoproteins) or less likely polymer. Latter conclusion was drawn from the fact that the application of 80 µg TPU monomer dissolved in chloroform also showed a spot at the point of application but of much weaker intensity. Moreover, TPU grafts showed significant degradation of material only after long-term implantation (12 months)[31] which pointed to the fact that the possible extraction of already degraded graft material can also be excluded. The assumption that these residues are polar lipids and not polymer material was moreover supported by the observation of similar spots in samples extracted from rat blood and aorta tissue. This finding also correlates with the proposed glycolayer formation on polymer materials[34], resulting in further increased hydrophilic material properties and, ultimately, better protein adsorption. It is also hypothesized that polar lipids are relevant for the change of blood-flow parameters and shear forces, depending on the type/degree of glycosylation.

For lipid analysis it was difficult to determine concentration differences in detail, and no obvious pattern change was observed after 7 days *in vivo* for TPU. Conversely, for ePTFE, higher intensities for cholesterol and phospholipids were observed. While it is not possible to match the applied lipid concentration (in analogy to matched protein concentrations for SDS-PAGE), the same volume of graft material was extracted, so it is possible to assume that the applied lipid content was comparable. Based on this assumption, the outstanding presence of cholesterol in TPU samples was explained by the pore size of the polymer graft, which is a few µm in size. The very likely happening cholesterol diffusion into the material may therefore be enhanced.

Analogous to protein analysis, PCA based on MS profiles of lipid extracts from polymer samples was performed. As only PC, SM and long chained glycosylated lipid species have been reported to be relevant for lubrication in the past,[35] other lipid species were excluded from the analysis. Lipids included in the analysis are listed in Fig. 7. Over 40 phospholipids from both graft materials and aorta tissue were assigned. Although statistical analysis was again capable of differentiating polymers and time points, no biological or material-related conclusions could be drawn from the cluster analysis. At this point it has to be stated that this study does not claim to be complete in respect to lipid identification and nature. Yet this analysis shows for the first time the most abundant lipid classes actually interacting with biomedical material *in vivo*. A large number of phospholipids

with long acyl chains were found alongside glycosylated lipids. This is in accordance with literature which describes in particular long-chained acyl chain compositions above 18 carbon atoms to be relevant for cell layer formation[36, 37].

Based on those findings, it is concluded that in comparison with ePTFE, the electrospinning process of TPU generates larger pores in the final vessel construct, thereby allowing better diffusion of cholesterol into the graft wall which enhances subsequent diffusion of other lipids and ultimately small proteins (*e.g* cytokines) into the vessel wall.

In vivo induced polymer modifications

In theory, disintegration of the biodegradable TPU begins with the hydrolysis of the ester bond, followed by the slower breakdown of the urethane linker. However, ePTFE contains one of the strongest existing organic bonds and is considered to be chemically inert; consequently, it is less likely to react with biological compounds. However, in the present study polymer modifications were found for both materials.

The pattern observed most frequently, with repeating units differing by Δm/z 24, were considered to be a carbon cluster induced by the laser fluence in the already damaged polymer areas. Previous MSI studies of polymers have correlated the presence of carbon clusters with a high sensitivity for laser irradiation[17]. These clusters correlated with lipid adsorption. For the analysed samples, it can be assumed that those areas are associated with either polymer degradation, or pore size enlargement and density reduction. ePTFE samples very rarely demonstrated Δm/z 137 and 170 modifications in defined areas, co-localized with phospholipid adsorption (Fig. 5). For TPU grafts, the following modifications were detected frequently: Δm/z 234, 248, 254, 264 and 268. As illustrated, the polymer modifications are distributed homogeneously across the entire analysed region, alongside classified lipid species. A homogeneous degradation or process of polymer change can be assumed; however, owing to the fact that all of the found polymer modifications have not yet been identified, further investigations are necessary.

CONCLUSIONS

The present study reveals the novelty of MSI in aiding the understanding the protein, peptide and lipid adsorption and diffusion behaviour that occurs with different graft materials that are used in vascular replacement systems. Owing to the very limited number of available explanted vessels, this presentation can be considered as a feasibility study, and the data interpretation must be considered

carefully. However, from experience, including other polymers interacting with the respective biological compartments, cholesterol adsorption and diffusion can be expected to be the initiating factors for a material's *in vivo* performance. In this study, cholesterol was the particular analyte, demonstrating significant differences for the biodegradable and the inert graft materials. The authors strongly believe that these molecules, and the associated protein complexes, are small enough to diffuse into the polymer vessels to initiate the formation of a biofilm, further enhancing protein adsorption and cell-layer formation. Additionally, the physico-chemical properties of TPU support this process in comparison with the more hydrophobic ePTFE. Future work will focus on the dynamic process of protein adsorption on graft materials by combining proteomics, lipidomics and MSI results. The authors strongly believe that this will help in enhancing the understanding of disadvantageous thrombosis formation and, consequently, biodegradable polymer design can be improved.

ACKNOWLEDGEMENTS

Parts of this project were supported by the Vienna University of Technology (Innovative Projects 2009/Chip-1000 and 2011/UltrafleXtreme III) and the Austrian Federal Ministry for Transport, Innovation and Technology (FFG project 826132/GENIE). The authors further acknowledge the COST Action BM1104 (Mass Spectrometry Imaging: New Tools for Healthcare Research) for valuable discussions. The authors highly appreciate the support of Prof. Günter Allmaier (Vienna University of Technology) for sharing his expertise and granting access to instrumentation.

FIGURE LEGENDS

Fig. 1 Polymer grafts and rat aorta were cut according to the scheme. Cross-sections, luminal and abluminal surfaces of centroid (C) and edge (E) regions were analyzed by mass spectrometry imaging.

Fig. 2 Protein adsorption on graft material: Mass spectrometric profiling of protein adsorption on (a) TPU and ePTFE after 10 min and 7 d and (b) the luminal surface of TPU; the protein names are tentatively assigned according to measured m/z values. Principal Component Analysis of obtained protein patterns (m/z 5000 – 80000, 28 features) reveals linear combinations of different markers separating clusters for (c) TPU and ePTFE surfaces and (d) *in vivo* times.

Fig. 3 Light microscopy images of ePTFE graft material after 10 min *in vivo* (luminal and abluminal surface) and aorta tissue are shown with corresponding MALDI images of median normalized intensity distribution of selected peptide and protein signals at a lateral resolution of 80 µm using SA/FA as matrix (a, b, c and d indicate the edges of the sample according to Fig. 1). Supporting material is available for unspecific protein distributions on luminal/abluminal ePTFE surfaces in comparison to aorta tissue but also for unspecific m/z distributions found on both materials, ePTFE and TPU.

Fig. 4 Protein separation, identification and functional classification. Protein extracts from ePTFE and TPU, after 10 min and 7 d *in vivo*, were separated by gel electrophoresis. Results are presented in comparison with protein extracts from the TPU center and edge. Protein identification is based on peptide mass fingerprinting and peptide sequencing. (protein abundance [ppm] in rat plasma is taken from PaxDb [30])

Fig. 5 Mass spectrometric imaging reveals the correlation of lipid adsorption and polymer modifications: distribution of PC(18:1/13:0) and PC(20:4/14:1) on the luminal surface of ePTFE and TPU grafts after different *in vivo* times. Polymer related signal distributions correlate with lipid localizations. Figures represent median normalized data at lateral resolutions of 150 µm for TPU and 30 µm for ePTFE.

Fig. 6 Cross-section analysis of a TPU graft (7 d *in situ*) reveals the diffusion of cholesterol into the vessel wall and polymer modification present in the graft wall. The vessel wall is approximately 80 µm thick and was imaged at a lateral resolution of 15 µm.

Fig. 7 Lipid separation and identification. Lipids extracted from aorta tissue, rat blood, ePTFE and TPU were separated by HP-TLC by repeated development (A – first development, B – second development) using two different mobile phases and Primuline staining. Lipids were identified directly from the TLC plate by MALDI-TOF/TOF-MS. To differentiate polymer residues from lipids, TPU monomer was dissolved in chloroform, deposited on the TLC plate and separated the same way.

REFERENCES

1. C. D. Stehouwer, D. Clement, C. Davidson, C. Diehm, J. W. Elte, M. Lambert, D. Sereni and E. V. M. W. Group, *Eur J Intern Med*, 2009, **20**, 132-138.
2. J. D. Kakisis, C. D. Liapis, C. Breuer and B. E. Sumpio, *J Vasc Surg*, 2005, **41**, 349-354.
3. L. E. Niklason and R. S. Langer, *Transpl Immunol*, 1997, **5**, 303-306.
4. F. E. Chlupac J, Bacakova L, *Physiol Res*, 2009, **58**, 119-139.
5. G. W. Bos, A. A. Poot, T. Beugeling, W. G. van Aken and J. Feijen, *Arch Physiol Biochem*, 1998, **106**, 100-115.
6. X. Wang, P. Lin, Q. Yao and C. Chen, *World J Surg*, 2007, **31**, 682-689.
7. A. W. Clowes, T. R. Kirkman and M. A. Reidy, *Am J Pathol*, 1986, **123**, 220-230.
8. R. Guidoin, S. Maurel, N. Chakfe, T. How, Z. Zhang, M. Therrien, M. Formichi and C. Gosselin, *Biomaterials*, 1993, **14**, 694-704.
9. D. Mantovani, P. Vermette, R. Guidoin and G. Laroche, *Biomaterials*, 1999, **20**, 1023-1032.
10. S. Lu, X. Sun, P. Zhang, L. Yang, F. Gong and C. Wang, *Perfusion*, 2013, **28**, 440-448.
11. F. J. Veith, S. Gupta and V. Daly, *Surgery*, 1980, **87**, 581-587.
12. R. J. Zdrahala, *J Biomater Appl*, 1996, **11**, 37-61.
13. M. Zhou, W. Qiao, Z. Liu, T. Shang, T. Qiao, C. Mao and C. Liu, *Tissue Eng Pt A*, 2014, **20**, 79-91.
14. A. W. Clowes and M. A. Reidy, *J Vasc Surg*, 1991, **13**, 885-891.
15. M. Casiano-Maldonado, G. T. Lim, X. P. Li, D. H. Reneker, J. E. Puskas and C. Wesdemiotis, *Int J Mass Spectrom*, 2013, **354**, 391-397.
16. D. V. Fröhlich SM, Archodoulaki V-M, Allmaier G, Marchetti-Deschmann M, *EuPA Open Proteomics*, 2014.
17. K. Krueger, C. Terne, C. Werner, U. Freudenberg, V. Jankowski, W. Zidek and J. Jankowski, *Anal Chem*, 2013, **85**, 4998-5004.
18. M. Marchetti-Deschmann and G. Allmaier, *J Mass Spectrom*, 2009, **44**, 61-70.
19. N. MWF, *Mass Spectrom Rev*, 1999, **18**, 309-344.
20. E. Pektok, B. Nottelet, J. C. Tille, R. Gurny, A. Kalangos, M. Moeller and B. H. Walpoth, *Circulation*, 2008, **118**, 2563-2570.
21. A. M. Seifalian, H. J. Salacinski, A. Tiwari, A. Edwards, S. Bowald and G. Hamilton, *Biomaterials*, 2003, **24**, 2549-2557.
22. D. F. Williams, *Biomaterials*, 2008, **29**, 2941-2953.
23. L. Xue and H. P. Greisler, *J Vasc Surg*, 2003, **37**, 472-480.

24. S. Baudis, S. C. Ligon, K. Seidler, G. Weigel, C. Grasl, H. Bergmeister, H. Schima and R. Liska, *Polym Sci A1*, 2012, **50**, 1272-1280.
25. C. Grasl, H. Bergmeister, M. Stoiber, H. Schima and G. Weigel, *J Biomed Mater Res A*, 2010, **93A**, 716-723.
26. S. C. Bergmeister H, Grasl C, Walter I, Plasenzotti R, Stoiber M, Bernhard D, Schima H, *Acta Biomater*, 2012, **9**, 6032-6040.
27. M. M. Bradford, *Anal Biochem*, 1976, **72**, 248-254.
28. D. N. Perkins, D. J. Pappin, D. M. Creasy and J. S. Cottrell, *Electrophoresis*, 1999, **20**, 3551-3567.
29. S. Fröhlich, V.-M. Archodoulaki, G. Allmaier and M. Marchetti Deschmann, *Anal Chem*, 2014, **86**, 9723-9732.
30. M. Wang, M. Weiss, M. Simonovic, G. Haertinger, S. P. Schrimpf, M. O. Hengartner and C. von Mering, *Mol Cell Proteomics*, 2012, **11**, 492-500.
31. H. Bergmeister, N. Seyidova, C. R. Schreiber, M. S. Strobl, C. Grasl, I. Walter, B. Messner, S. Baudis, S. Fröhlich, M. Marchetti Deschmann, M. Griesser, M. di Franco, M. Krssak, R. Liska and H. Schima, *Acta Biomater*, 2015, **11**, 104-113.
32. E. J. Cho, Z. Tao, Y. Tang, E. C. Tehan, F. V. Bright, W. L. Hicks, Jr., J. A. Gardella, Jr. and R. Hard, *J Biomed Mater Res A*, 2003, **66**, 417-424.
33. P. Vermette, D. Mantovani, R. Guidoin, J. Thibault and G. Laroche, *J Vasc Surg*, 1998, **28**, 527-534.
34. T. M. Allen, *Adv Drug Deliver Rev* , 1994, **13**, 285-309.
35. V. Pengo, A. Biasiolo, T. Brocco, S. Tonetto and A. Ruffatti, *Thromb Haemostasis*, 1996, **75**, 721-724.
36. R. Schneiter, B. Brugger, C. M. Amann, G. D. Prestwich, R. F. Epand, G. Zellnig, F. T. Wieland and R. M. Epand, *The Biochemical Journal*, 2004, **381**, 941-949.
37. L. Bach, L. Gissot, J. Marion, F. Tellier, P. Moreau, B. Satiat-Jeunemaitre, J. C. Palauqui, J. A. Napier and J. D. Faure, *J Cell Sci*, 2011, **124**, 3223-3234.

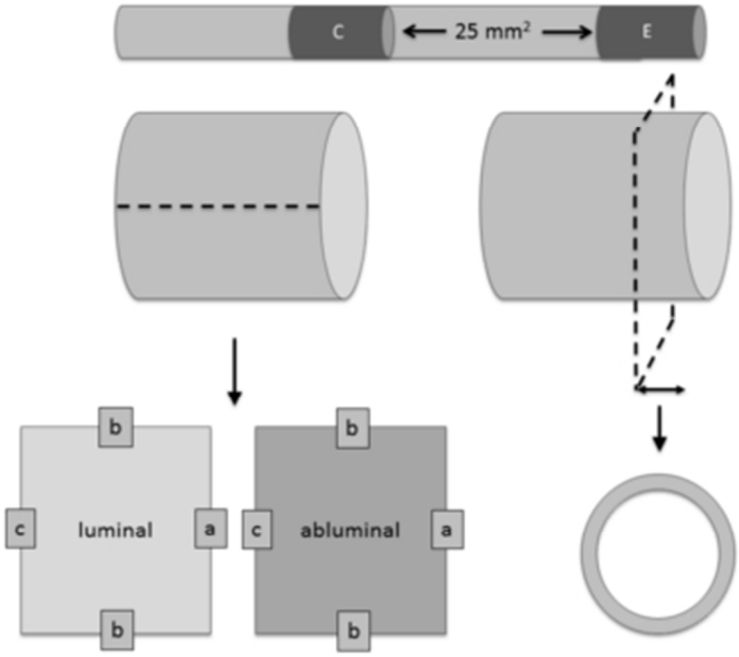

Polymer grafts and rat aorta were cut according to the scheme. Cross-sections, luminal and abluminal surfaces of centroid (C) and edge (E) regions were analyzed by mass spectrometry imaging
102x89mm (96 x 96 DPI)

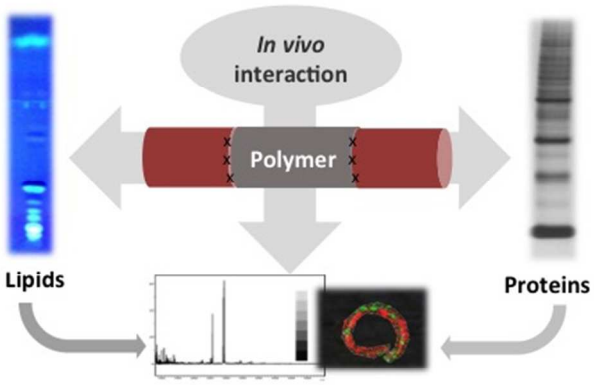

Graphical Abstract
254x142mm (72 x 72 DPI)

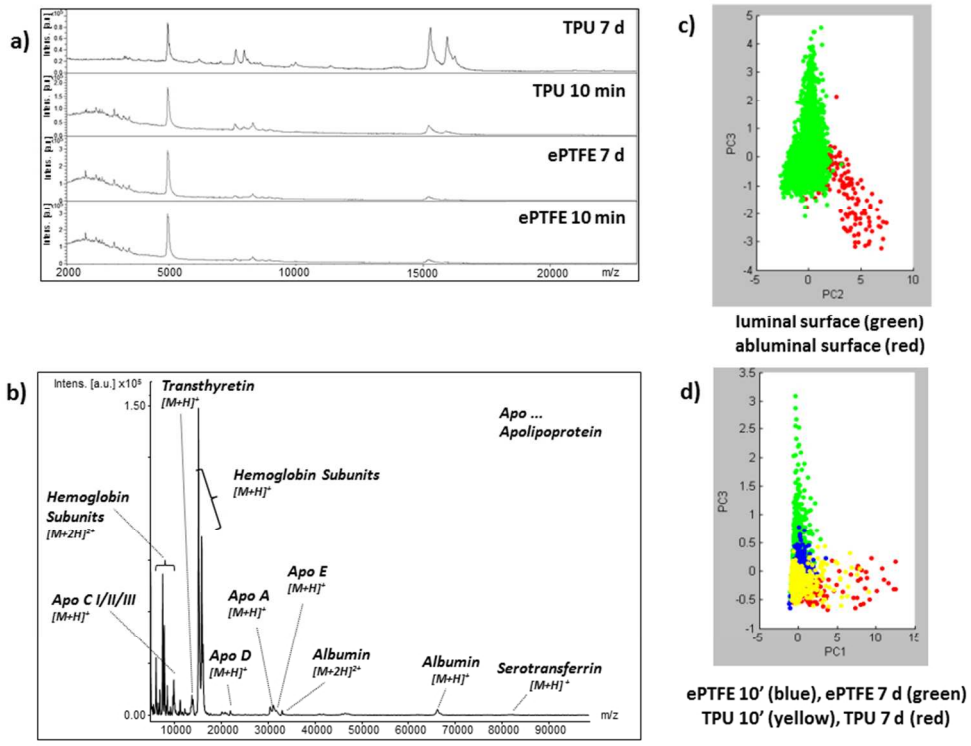

Protein adsorption on graft material: Mass spectrometric profiling of protein adsorption on (a) TPU and ePTFE after 10 min and 7 d and (b) the luminal surface of TPU; the protein names are tentatively assigned according to measured m/z values. Principal Component Analysis of obtained protein patterns (m/z 5000 – 80000, 28 features) reveals linear combinations of different markers separating clusters for (c) TPU and ePTFE surfaces and (d) in vivo times
254x190mm (96 x 96 DPI)

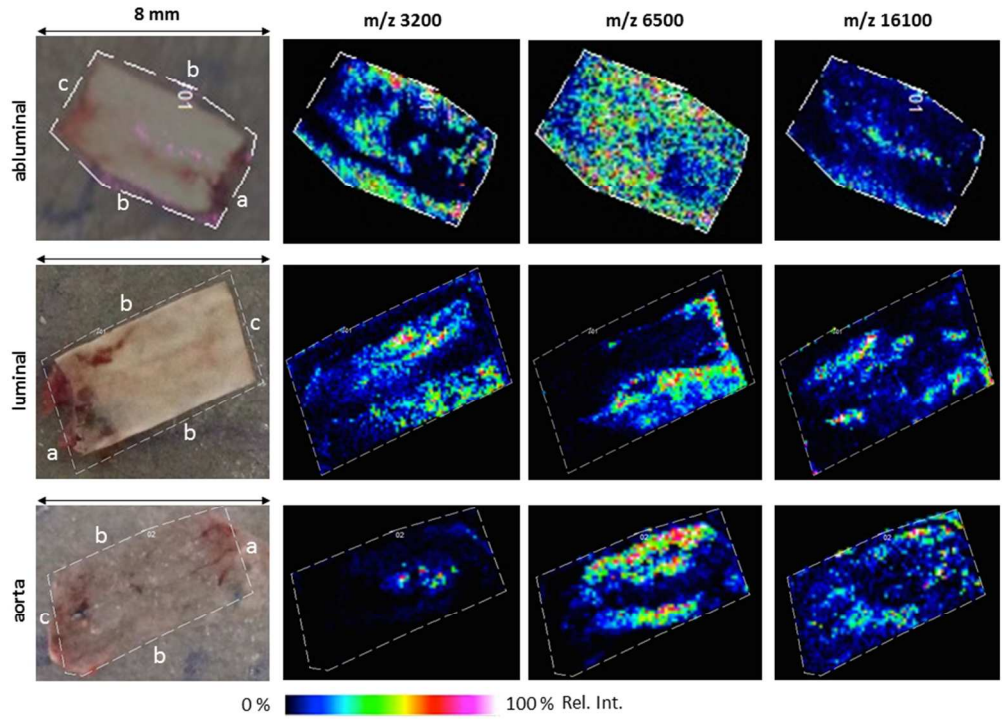

Light microscopy images of ePTFE graft material after 10 min in vivo (luminal and abluminal surface) and aorta tissue are shown with corresponding MALDI images of median normalized intensity distribution of selected peptide and protein signals at a lateral resolution of 80 µm using SA/FA as matrix (a, b, c and d indicate the edges of the sample according to Fig. 1). Supporting material is available for unspecific protein distributions on luminal/abluminal ePTFE surfaces in comparison to aorta tissue but also for unspecific m/z distributions found on both materials, ePTFE and TPU
254x190mm (96 x 96 DPI)

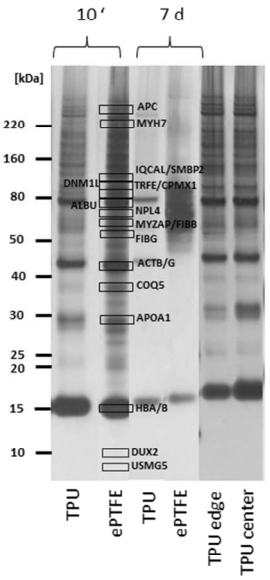

Protein	Abbreviation	Nominal mass [Da]	Functional classification	Plasma abundance [ppm]
Myosin-7	MYH7_RAT	223083	muscle contraction	54
Adenomatous polyposis coli protein	APC_RAT	310533	cell migration	8
Up-regulated during skeletal muscle growth protein 5	USMG5_RAT	6460	sceletal muscle growth	170
Putative double homeobox protein	DUX2_RAT	9312	DNA binding	no information
Hemoglobin subunit alpha-1/2	HBA_RAT	15490	O2 transport	3493
Hemoglobin subunit b1	HBB1_RAT	16083	O2 transport	6088
Hemoglobin subunit beta-2	HBB2_RAT	16086	O2 transport	
Apolipoprotein A-I	APOA1_RAT	30759	cholesterol transport	11
2-methoxy-6-polyprenyl-1,4-benzoquinol methylase	COQ5_RAT	37402	metabolism	13
Actin	ACTB_RAT	42052	cell motility	13073
Actin, cytoplasmic 2	ACTG_RAT	42108	cell motility	13270
Fibrinogen gamma chain	FIBG_RAT	51228	platelet aggregation	153
Myocardial zonula adherens protein	MYZAP_RAT	54093	cell maturation	no information
Fibrinogen beta chain	FIBB_RAT	54828	platelet aggregation	168
Nuclear protein localization protein 4 homolog	NPL4_RAT	68982	cell division	2
Albumin	ALBU_RAT	70682	transport/blood pressure	4505
Serotransferrin	TRFE_RAT	79294	transport/stimulating cell proliferation	572
Probable carboxypeptidase X1	CPXM1_RAT	82243	cell-cell interaction	3
Dynamin 1 like protein	DNM1L	84369	cell proliferation	28
IQ and AAA domain-containing protein 1-like	IQCAL_RAT	95964	cell division	1
DNA-binding protein SMUBP-2	SMBP2_RAT	109994	transcription regulator	no information

Protein separation, identification and functional classification. Protein extracts from ePTFE and TPU, after 10 min and 7 d in vivo, were separated by gel electrophoresis. Results are presented in comparison with protein extracts from the TPU center and edge. Protein identification is based on peptide mass fingerprinting and peptide sequencing. (protein abundance [ppm] in rat plasma is taken from PaxDb 30)
254x190mm (96 x 96 DPI)

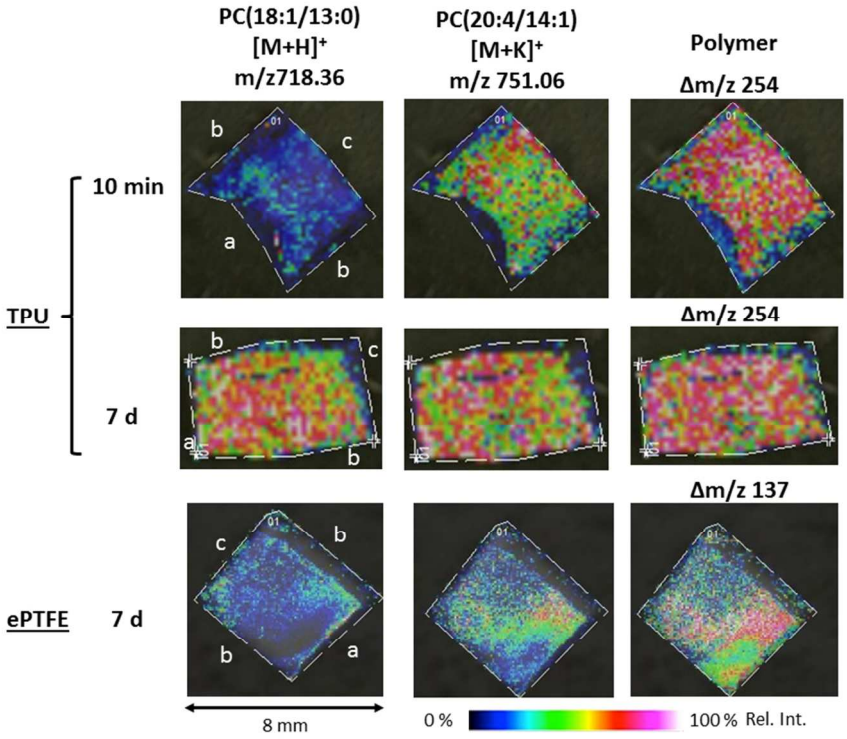

Mass spectrometric imaging reveals the correlation of lipid adsorption and polymer modifications: distribution of PC(18:1/13:0) and PC(20:4/14:1) on the luminal surface of ePTFE and TPU grafts after different in vivo times. Polymer related signal distributions correlate with lipid localizations. Figures represent median normalized data at lateral resolutions of 150 µm for TPU and 30 µm for ePTFE
254x190mm (96 x 96 DPI)

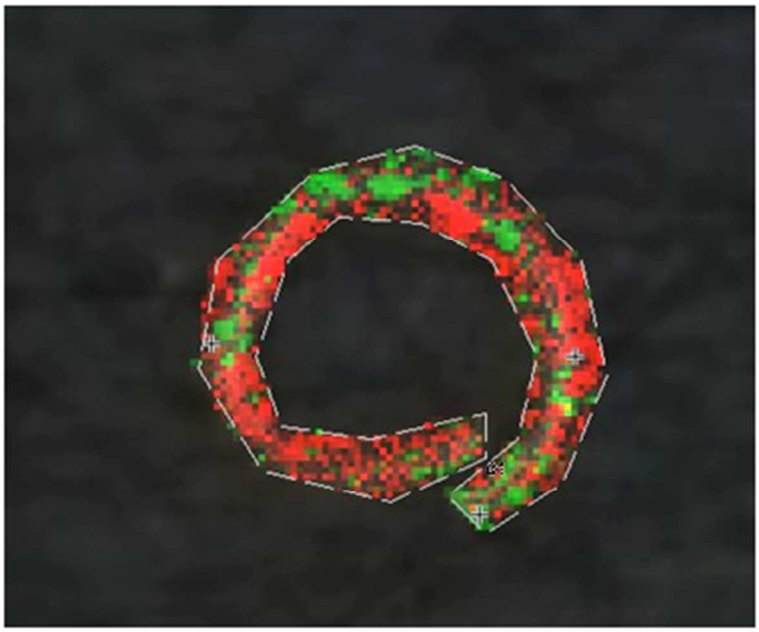

Cross-section analysis of a TPU graft (7 d in situ) reveals the diffusion of cholesterol into the vessel wall and polymer modification present in the graft wall. The vessel wall is approximately 80 μm thick and was imaged at a lateral resolution of 15 μm
106x99mm (96 x 96 DPI)

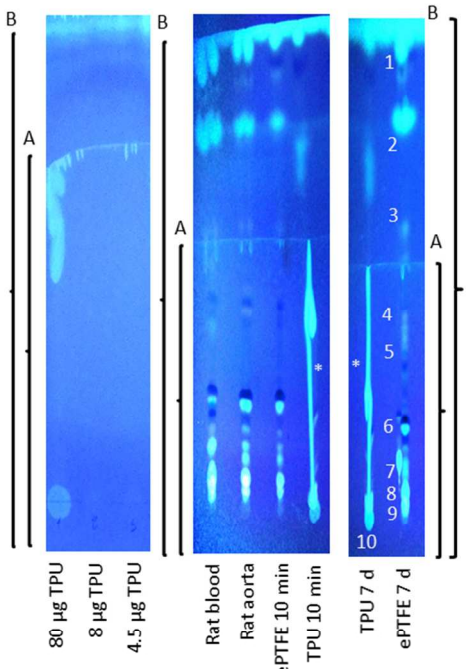

	Species	Acyl Chain
1	Ceramides, apolar lipids	18:0/18:0, 18:1/18:0, 18:1/18:1, 20:2/18:0, 20:2/18:1, 22:0/18:0, 22:2/18:0
2	Triglycerides	54:4, 54:6, 60:4, 60:6
3	Cholesterol	
4	Phosphatidyl ethanol-amine	16:0, 18:0, 18:1, 18:2, 16:0/16:0, 16:0/18:0, 18:0/18:0, 18:0/18:1, 18:0/18:2, 18:1/18:1, 18:2/18:2, 20:0/18:0, 20:0/18:1, 20:0/18:2, 20:1/18:0, 20:1/18:1, 20:4/18:0, 20:4/18:1
5	Phosphatidyl-inositol	16:0, 18:0, 18:0/16:0, 18:0/18:0, 18:1/18:0, 18:2/18:0, 20:4/18:0, 22:0/18:0
6	Phosphatidyl-serine	16:0, 18:0, 18:1, 18:2, 18:0/16:0, 18:1/16:0, 18:2/16:0, 18:0/18:1, 18:1/18:1, 20:2/18:0, 20:2/18:1
7	Sphingo-myelin	18:0/16:0, 18:1/16:0, 18:2/16:0, 20:0/18:0, 20:1/18:0, 22:0/18:0, 22:0/18:1, 22:1/18:1, 24:0/18:1, 24:1/18:1
8	Phosphatidyl-choline	16:0/16:0, 18:0/16:0, 18:1/13:0, 18:1/16:0, 18:0/18:0, 18:1/18:1, 18:1/18:2, 18:2/18:0, 20:0/16:0, 20:0/18:0, 20:0/20:0, 20:1/18:0, 20:1/20:1, 20:2/18:0, 20:2/18:1 20:4/14:1, 20:4/18:0, 20:4/18:1
9	Lyso-phosphatidyl-choline	16:0, 18:0, 18:1, 18:2, 20:0
10	polar extractable compounds	
*	Cholesterol traces	

254x190mm (96 x 96 DPI)